Available online at www.sciencedirect.com

ScienceDirect

Scripta Materialia 99 (2015) 93–96

Scripta MATERIALIA

www.elsevier.com/locate/scriptamat

The use of high-entropy alloys in additive manufacturing

Yevgeni Brif, Meurig Thomas and Iain Todd*

Department of Materials Science and Engineering, University of Sheffield, Mappin Street, Sheffield S1 3JD, UK

Received 3 November 2014; revised 26 November 2014; accepted 30 November 2014
Available online 17 December 2014

An equiatomic FeCoCrNi high-entropy alloy is used as an input material for selective laser melting. The material is characterized using X-ray diffraction, scanning electron microscopy, thermal analysis and mechanical testing to investigate the feasibility of using high-entropy alloys in additive manufacturing and the resulting tensile properties. Results show that not only does the alloy preserve its single-phase solid-solution state, but it also exhibits high strength and ductility that are comparable to engineering materials like stainless steels.

Keywords: High-entropy alloys; Laser deposition; Tension test; XRD

Since high-entropy alloys (HEAs) were first reported 10 years ago [1,2], they have attracted significant attention from researchers globally [3,4]. As the potential for major developments using conventional alloy design is decreasing, HEAs show considerable promise from both a scientific and an application perspective. The generally accepted definition of an HEA is that it is a system of five or more principal elements, each having a concentration between 5 and 35 at.%. As a result of the multi-component nature of HEA systems, they are expected to exhibit a complex microstructure with various phases and intermetallics. This is not always the case, however; the microstructure of HEAs is a simple, single-phase solid solution, and, although the majority of current research is focused on equimolar systems containing five or more principal elements, the characteristic high-entropy microstructure has also been reported for both non-equimolar systems [5] and for four-component alloys [6,7].

The underlying mechanism behind the HEAs is a minimization of the Gibbs free energy through a balance between entropy and enthalpy [8]. The vast number of possible alloy combinations and the possibility of tailoring the constituent elements to tune the final properties of the HEA are the two major reasons for the increasing scientific attention in this field. Despite the growing interest in HEAs, most published works focus mainly on the thermodynamic aspects of HEAs and the resulting microstructure. Although data pertaining to the mechanical properties of HEAs are available in the literature, at present it is largely limited to monotonic compressive loading and bulk hardness testing [9–11].

Recently, the tensile properties of various HEA systems have been reported, indicating that they are extremely ductile and can be work hardened [5,7,12,13]. With the exception of the work of Kunce et al. [14] and works involving HEA coatings prepared by laser cladding [15,16], all currently published works utilized arc melting or an induction furnace followed by casting to produce the high-entropy alloys: these methods are unlikely to present an industrially suitable route for the production and use of HEAs. As these alloys are relatively complex systems, it is safe to assume that their implementation will be limited to highly demanding applications, where the potential benefit of HEAs will overcome the inherent complexity and high levels of control required to produce them. With this in mind, it would appear that additive manufacturing (AM), which facilitates a high level of local process control and generates rapid solidification cooling rates, may be a suitable candidate for utilizing HEAs as an engineering material. This research was conducted with two major aims: to demonstrate the feasibility of producing HEAs via an AM route and yo report the mechanical properties of a four-component FeCoCrNi HEA produced by AM.

In order to address the first research aim, selective laser melting (SLM) was chosen as the AM method in this research. SLM is one of the most popular and widespread of the AM methods. As such, it is a good starting point for exploring these new alloys.

The AM specimens were manufactured from pre-alloyed, gas-atomized FeCoCrNi powder, the chemical composition of which is provided in Table 1. All specimens were manufactured using a Renishaw SLM125 machine with a maximum laser intensity of 200 W and a laser spot size of 50 μm. Two different specimen geometries were used: 10 mm cubic specimens were manufactured for thermal analysis, metallography and hardness testing, while a set of 8 mm × 8 mm × 60 mm cubic coupons were produced

* Corresponding author; e-mail: i.todd@sheffield.ac.uk

http://dx.doi.org/10.1016/j.scriptamat.2014.11.037
1359-6462/

Table 1. Chemical composition of powder, analysed using XRF (AMG Superalloys UK).

Element	Fe	Co	Cr	Ni	Al	Si	Zr	Other
wt.%	23.48	26.28	21.07	27.16	0.14	0.1	0.11	<0.05

as blanks for tensile testing. Each set of specimens were analysed (i) in the as-deposited state and (ii) after two different homogenization treatments: for 12 h at 750 and 1000 °C, followed by water quenching. To benchmark the FeCoCrNi manufactured by laser powder bed processing, a small number of 9 mm diameter cast specimens of identical composition were produced using an Edmund Buhler MAM-1 electric arc melter with a water-cooled copper mould.

The effect of processing parameters on the microstructure and properties is emphasized in powder-bed AM technologies, as the fusion between the deposited powder layers depends on the melt penetration depth of the laser beam. If the powder bed layer thickness is greater than the depth of the melt pool, the layer will not be completely melted and only partial inter-layer bonding will be achieved. In the absence of a robust process parameter set for selective laser melting of FeCoCrNi powder, we employed a numerical approach based on the Rosenthal model [17] (see e.g. Eq. (1) in Ref. [18]) to provide an initial prediction for the melt penetration depth as a function of laser beam power, q (W), and velocity, v (m s^{-1}). For the purpose of these preliminary calculations, the laser beam power was fixed at the maximum available for the Renishaw SLM125 platform of $q = 200$ W and, based on previous analysis by Deffley [19], the fraction of absorbed beam power was estimated to be 0.25. The powder bed substrate was fixed at room temperature and the beam velocity was set to $v = 0.3$ m s^{-1}.

In order to accurately simulate the melt pool geometry using the Rosenthal model, the material thermal properties are required. As physical property data are not readily available for this alloy, the thermal conductivity was assumed to lie in the range $80<k<100$ W m^{-1} K^{-1}, which is within the thermal conductivity range of the constituent elements. As the measured specific heat capacity ($C_p = 444$ J kg^{-1} K^{-1} at 25 °C) for the FeCoCrNi alloy, obtained through differential scanning calorimetry (DSC) analysis, was similar to the values of the base elements, we believe this assumption to be reasonable for this work. Several numerical calculations were conducted using the Scilab software [20], in which the thermal conductivity (k) value was varied between 80 and 100 W m^{-1} K^{-1} and the melt pool depth was predicted to be in the range 45–50 μm.

On the basis of these estimated melt pool depths, two groups of specimens were manufactured. One, representing the worst-case scenario, was manufactured using a 50 μm layer thickness, right on the limit of the simulated penetration depth. The second type, representing the best-case scenario, was manufactured using a 20 μm layer thickness, which is the thinnest layer possible on the SLM device used.

Phase characterization was performed by X-ray diffraction (XRD) using a Siemens D5000 Bragg–Brentano diffractometer, with a Cu K_α radiation source ($\lambda = 1.54$ Å). Thermal stability, specific heat capacity and thermal expansion were measured using differential thermal analysis (DTA), DSC and thermomechanical analysis (TMA), respectively. DTA experiment was performed in a Perkin Elmer STA8000 machine between 40 and 1450 °C, with a heating rate of 10 °C min^{-1}. The specific heat capacity was measured using a Perkin Elmer Diamond differential scanning calorimeter between 20 and 590 °C, with a heating rate of 20 °C min^{-1}. The thermal expansion coefficient was measured using a Perkin Elmer Pyris diamond thermomechanical analyser between 25 and 500 °C, with a heating rate of 5 °C min^{-1}.

Mechanical testing was performed in accordance with ASTM E8 M at Element Materials Technology, Sheffield, UK, using round tensile bars of 20 mm gauge length and 4 mm diameter. Vickers hardness testing was performed using a Struers DuraScan automated indenter (1 kg.f load), with at least 20 measurements per sample.

Microstructural studies and chemical analysis of the SLM specimens were performed using an FEI Inspect-F scanning electron microscope equipped with an EDAX energy-dispersive X-ray spectroscopy (EDS) detector. Both as-deposited and homogenized specimens were analysed. Specimens for microstructure analysis were sectioned, mounted and prepared via a standard mechanical grinding and polishing route. The size distribution of internal porosity was measured by examining a number of 2-D planar cross-sections using light optical microscopy and employing an automated thresholding procedure in the image analysis software ImageJ.

The XRD patterns (Fig. 1) indicate that all four specimens possess a single-phase face-centred cubic (fcc) crystal structure, with $a \approx 3.58$ Å. Comparable XRD results were also obtained for specimens manufactured using beam traverse rates of 0.33, 0.36, 0.38, 0.44, 0.48 and 0.5 m s^{-1}, which indicates that a single-phase solid solution is obtainable across a range of processing parameters. DTA was used to confirm the stability of the single-phase solid solution and to obtain the melting point of this HEA. The DTA results are presented in Figure 2. It is clear from the DTA

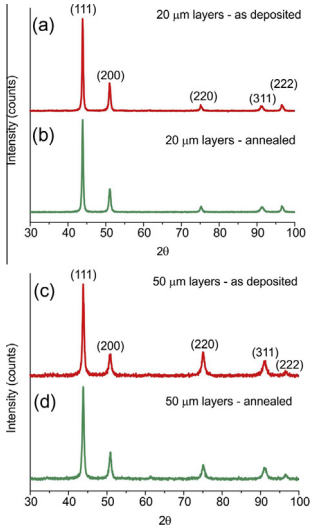

Figure 1. XRD patterns of SLM manufactured FeCoCrNi alloy: (a) 50 μm as-deposited specimen, (b) 50 μm annealed specimen, (c) 20 μm as-deposited specimen and (d) 20 μm annealed specimen.

data that no phase transformations take place up to the melting point of the alloy (1414 °C). The specific heat capacity ($C_p = 444$ J kg^{-1} K^{-1} at 25 °C) was obtained using DSC. Further thermal analysis, using TMA, provided values for the coefficient of thermal expansion (CTE $= 1.65 \times 10^{-5}$ K^{-1}) for the FeCoCrNi HEA. Both the specific heat capacity and the thermal expansion values are similar to the values of the constituent elements.

The microstructure of the 20 μm layer specimen is given in Figure 3, while the inset shows the EDS elemental maps. The subtle variations in greyscale across the backscattered electron micrograph are due to the electron channelling contrast between adjacent FeCoCrNi grains of dissimilar crystallographic orientation with respect to the specimen surface. The EDS signals reveal a uniform chemical composition with no visible segregation. No changes in chemical uniformity were observed after annealing for 12 h at 750 °C.

Representative engineering stress–strain curves for the tensile specimen manufactured using a layer thickness parameter of 20 μm is presented in Figure 4a. It is clear from the results that this HEA is highly ductile, as expected from an fcc alloy, while still retaining high strength. The tensile properties of the material produced using a 50 μm layer thickness were inferior to the 20 μm example and were characterized by a significantly lower proof strength and reduced ductility (Table 2). This latter result is to be very much expected as the laser beam melt penetration depth was insufficient to fully fuse the 50 μm thick layers, leading to an increase in both the size and frequency of internal, melt-related defects (Fig. 4b).

To compare the mechanical properties of the AM specimens with a more traditional processing route, tensile testing was performed on an FeCoCrNi HEA manufactured using arc melting and casting. As the results obtained for the arc melted specimens were in excellent agreement with the results of Salishchev et al. [7], they were used as a reference point in this work. To further explore the mechanical properties, microhardness tests were also carried out on both types of AM specimens, as well as on the arc melted sample. The results of the AM and arc melted specimens are presented in Table 2.

We should point out that, due to the inherent problems with fusion in the 50 μm specimens described before, these specimens do not represent the true mechanical properties of this alloy, and the discussion will focus on the 20 μm specimens from this point onwards.

Table 2 shows that the yield strength obtained using SLM (600 MPa) is more than three times higher than that achieved using arc melting and casting (188 MPa). This major increase in strength was achieved while maintaining

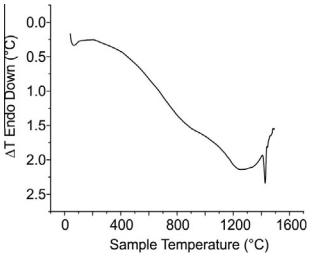

Figure 2. Differential thermal analysis of the FeCoCrNi high-entropy alloys manufactured by selective laser melting.

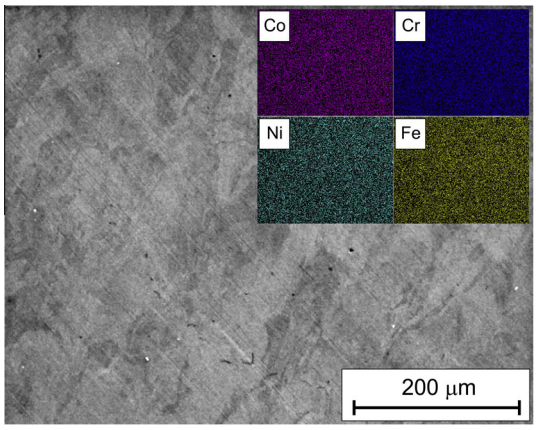

Figure 3. As-deposited microstructure: SE image of a 20 μm specimen. The inset shows EDS element maps of the same area.

a significant portion of the alloy's ductility. As AM processes produce net-shape products, the use of work hardening methods to improve the mechanical properties of the part is not possible. Consequently, parts manufactured using AM can be used only in the as-deposited state or the heat-treated state.

After annealing at 750 °C, a reduction in yield and tensile strength (to 495 and 695 MPa, respectively) was observed, with a minor reduction in ductility (30%). This reduction in strength is a result of stress relief. After fabrication in SLM, the part contains residual stresses, which are removed as a result of the annealing treatment. The increased annealing temperature caused a combined effect of stress relief and grain growth. This combined effect reduced the yield and tensile strength of the material (to 433 and 682 MPa, respectively), while the ductility of the material increased (42%). It is possible that a more prolonged heat treatment, or a higher temperature, will cause a more significant change in the tensile properties. However, no such precipitation has been reported for this HEA, meaning that precipitation hardening is unlikely to happen in this case.

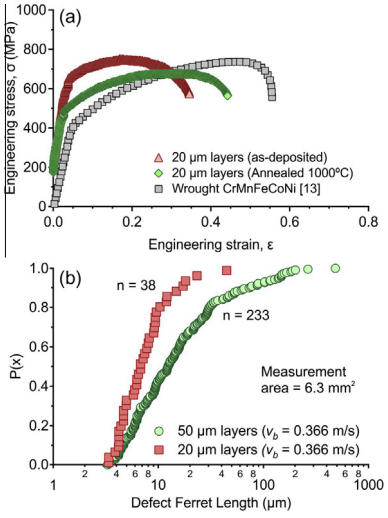

Figure 4. (a) Representative tensile curves for 20 μm layer thickness AM specimens and (b) empirical cumulative probability distributions of the population of observed defects in the SLM FeCoCrNi HEA manufactured using a layer thickness of (i) 20 μm and (ii) 50 μm.

Table 2. Tensile and hardness results of the AM and arc melted specimens.

Specimens		$\sigma_{0.2}$ (MPa)	UTS (MPa)	Elongation (%)	HV 1
Arc melter	As-Cast	188	457	50	118
AM 50 μm	As-Deposited	402	480	8	205
AM 20 μm	As-Deposited	600	745	32	238

The significantly enhanced mechanical properties of the AM specimens, as compared to cast samples, are attributed to the fine microstructure obtained in SLM. The large amount of energy used to melt thin layers of powder creates large temperature gradients and rapid solidification, resulting in fine grains. The influence of grain size on the tensile properties of HEAs was previously shown by Otto et al. [21]. The strong Hall–Petch effect, combined with the lack of any brittle intermetallics or second phases, enables the FeCoCrNi HEA to possess high strength and good ductility at the same time. In fact, when compared to commercially available stainless steel alloys, as well as stainless steels processed by SLM [22], the described HEA, manufactured using SLM, shows similar mechanical properties.

The results of this work clearly demonstrate that not only can high-entropy alloys be used in SLM, but also that the obtained mechanical properties make them a viable material for engineering applications. To the best of our knowledge, this is the first work to successfully use an HEA in AM. And, despite further study is necessary for this specific alloy, the initial results are extremely promising. It is our belief that the ever-increasing interest in HEAs will lead to the development of novel alloys of engineering importance. These new alloys, combined with the option to use them in advanced manufacturing processes like AM, will open the door to a new world of opportunities.

The authors would like to thank James Hunt, Neil J. Harrison and Ioannis Violatos for their contributions.

[1] J.W. Yeh, S.K. Chen, S.J. Lin, J.Y. Gan, T.S. Chin, T.T. Shun, C.H. Tsau, S.Y. Chang, Adv. Eng. Mater. 6 (2004) 299–303.
[2] B. Cantor, I.T.H. Chang, P. Knight, A.J.B. Vincent, Mater. Sci. Eng., A 375–377 (2004) 213–218.
[3] Y. Zhang, T.T. Zuo, Z. Tang, M.C. Gao, K.A. Dahmen, P.K. Liaw, Z.P. Lu, Prog. Mater. Sci. 61 (2014) 1–93.
[4] M. Gao, D. Alman, Entropy 15 (2013) 4504–4519.
[5] M.J. Yao, K.G. Pradeep, C.C. Tasan, D. Raabe, Scr. Mater. 72–73 (2014) 5–8.
[6] Z. Wu, H. Bei, F. Otto, G.M. Pharr, E.P. George, Intermetallics 46 (2014) 131–140.
[7] G.A. Salishchev, M.A. Tikhonovsky, D.G. Shaysultanov, N.D. Stepanov, A.V. Kuznetsov, I.V. Kolodiy, A.S. Tortika, O.N. Senkov, J. Alloy. Compd. 591 (2014) 11–21.
[8] F. Otto, Y. Yang, H. Bei, E.P. George, Acta Mater. 61 (2013) 2628–2638.
[9] C.-C. Juan, C.-Y. Hsu, C.-W. Tsai, W.-R. Wang, T.-S. Sheu, J.-W. Yeh, S.-K. Chen, Intermetallics 32 (2013) 401–407.
[10] X. Yang, Y. Zhang, P.K. Liaw, Procedia Eng. 36 (2012) 292–298.
[11] Y. Dong, Y. Lu, J. Kong, J. Zhang, T. Li, J. Alloy. Compd. 573 (2013) 96–101.
[12] A. Gali, E.P. George, Intermetallics 39 (2013) 74–78.
[13] B. Gludovatz, A. Hohenwarter, D. Catoor, E.H. Chang, E.P. George, R.O. Ritchie, Science 345 (2014) 1153–1158.
[14] I. Kunce, M. Polanski, J. Bystrzycki, Int. J. Hydrogen Energy 38 (2013) 12180–12189.
[15] H. Zhang, Y. Pan, Y. He, H. Jiao, Appl. Surf. Sci. 257 (2011) 2259–2263.
[16] H. Zhang, Y. Pan, Y.-Z. He, Mater. Des. 32 (2011) 1910–1915.
[17] D. Rosenthal, Trans. ASME 11 (1946) 849–866.
[18] S.S. Al-Bermani, M.L. Blackmore, W. Zhang, I. Todd, Metall. Mater. Trans. A 41 (2010) 3422–3434.
[19] R. Deffley, Development of Processing Strategies for the Additive Layer Manufacture of Aerospace Components in Inconel 718 (PhD Thesis), Department of Materials Science and Engineering, University of Sheffield, 2012.
[20] S. Enterprises, Scilab Enterprises, Orsay, France, 2012.
[21] F. Otto, A. Dlouhý, C. Somsen, H. Bei, G. Eggeler, E.P. George, Acta Mater. 61 (2013) 5743–5755.
[22] I. Tolosa, F. Garciandía, F. Zubiri, F. Zapirain, A. Esnaola, Int. J. Adv. Manuf. Technol. 51 (2010) 639–647.